Hindawi
Scientific Programming
Volume 2021, Article ID 9899036, 9 pages
https://doi.org/10.1155/2021/9899036

Research Article

MRI Findings of Acute Sports Injury of the Gastrocnemius Muscle

Li Xue

Zibo Vocational College, Zibo New District, Shandong 255314, China

Correspondence should be addressed to Li Xue; 0013010@yzpc.edu.cn

Received 22 June 2021; Accepted 18 August 2021; Published 16 September 2021

Academic Editor: Gustavo Ramirez

*Objective.*To investigate the MRI findings of acute sports injury of the gastrocnemius muscle and to provide evidence for clinical diagnosis. *Methods*. The MRI imaging data of 16 cases of gastrocnemius muscle group sports injury were compared, analyzed, and collated. In this paper, the variation of MRI image entropy before and after gastrocnemius muscle injury was studied by using the texture characteristics of the muscle image. *Results*. The experiment demonstrated that the entropy of MRI images before and after fatigue showed a decrease after muscle tissue was raised; that is, after muscle tissue underwent centrifugal and centripetal contraction. This result is more effective and convenient for nondestructive prediction of the gastrocnemius muscle injury state. *Conclusion*. MRI can show the site and pathological changes of acute gastrocnemius injury.

1. Introduction

Gastrocnemius motor injury is a common injury among lower limb motor injuries. Ultrasound and other imaging methods play a role in the detection of acute sports injury of the gastrocnemius muscle [1, 2]. Magnetic resonance imaging (MRI) has good soft tissue resolution, for soft tissue injury, edema, and hemorrhage, according to its characteristics, and the calf muscles injury also exhibit certain MRI features. MRI can show the skin, subcutaneous shallow deep fascia, muscles, tendon, ligament, joint capsule, synovial sheath, and slippery bursa and bone pathological damage. It is of great significance to understand the pathogenesis of this injury and the scope and degree of injury involvement [3]. In this paper, we analyzed the MRI signs of 16 cases of gastrocnemius muscle group sports injury admitted to our hospital from January 2016 to January 2020 and discussed the imaging findings of this disease. 16 normal gastrocnemius groups were tested, and the following data were obtained.

2. Materials and Methods

2.1. Clinical Data. Among the 16 patients, there were 8 males and 8 females. The clinical manifestations were mainly leg pain after exercise. The X-ray plain film showed no signs of lower limb fracture. MRI showed sural injury, and the clinical and imaging diagnosis was acute gastrocnemius injury. The author observed, analyzed, and summarized the imaging signs of its clinical manifestations. The main reasons for sports injuries: playing basketball and other jumping and leaping sports and also some running or rushing. Most patients are injured when they are forced and hear the sudden short “click” sound of the small leg, and then, there is severe pain, swelling, and gradual aggravation, leading to difficulties in walking, lameness, and other movement disorders. Physical examination showed swelling at the back of the leg, subcutaneous ecchymosis, obvious tenderness in the part, and obvious pulling pain during toe movement [4]. Plain X-ray examination was performed 1–3 days after the injury, and MRI examination was performed 1–10 days after the injury.

2.2. MRI. The lower leg MRI was performed with a Magnetomc0.35 T open magnetic resonance imaging system of Siemens and Avanto 1.5 T superconducting magnetic resonance imaging system of Siemens, or GE SignaExcite 0.35T Magnetic Resonant Imaging System. The imaging coil is selected from the knee joint phased-front coil, and the imaging sequences included sagittal T1-weighted images (TR414 ms and TE15 ms), T2-weighted images (TR3520 ms

Table 1: Maximum heel lifting strength of 16 male subjects (unit: kg).

Males	Subject 1	Subject 2	Subject 3	Subject 4	Subject 5	Subject 6	Subject 7	Subject 8
Test 1	31.75	32.20	29.48	32.20	30.08	29.48	32.20	34.01
Test 2	32.65	32.20	29.48	31.75	30.39	29.92	32.20	34.01
Test 3	31.75	31.75	29.02	32.20	30.08	29.48	32.65	32.65
Average	32.02	32.06	29.34	23.02	32.02	29.61	32.34	33.56

Table 2: Maximum heel lifting strength of 16 female subjects (unit: kg).

Females	Subject 1	Subject 2	Subject 3	Subject 4	Subject 5	Subject 6	Subject 7	Subject 8
Test 1	22.67	23.58	21.31	19.50	20.41	23.13	20.86	22.22
Test 2	23.13	24.04	20.86	19.50	20.41	23.13	20.86	21.77
Test 3	22.67	23.58	21.31	19.05	20.86	23.58	20.41	22.22
Average	22.81	23.72	21.13	19.32	20.54	23.26	20.68	22.04

Table 3: The number of heel lifts (units) in male subjects was dense to the muscle injury.

Males	There is no load	20% MVCT	30% MVCT	40% MVCT
Subject 1	10	10	10	10
Subject 2	16	14	12	16
Subject 3	12	14	14	12
Subject 4	10	12	14	12
Subject 5	10	10	9	7
Subject 6	16	10	10	12
Subject 7	12	14	16	12
Subject 8	12	14	14	12

Table 4: The number of heel lifts (units) in female subjects was dense to the muscle injury.

Males	There is no load	20% MVCT	30% MVCT	40% MVCT
Subject 1	12	12	14	12
Subject 2	16	14	16	14
Subject 3	16	12	14	8
Subject 4	12	14	12	14
Subject 5	16	12	12	14
Subject 6	14	14	12	14
Subject 7	14	12	14	10
Subject 8	14	14	12	12

and TE90 ms) and fat-inhibitory or water-activated sequences (TR601 ms and TE24.4 ms), and axial T2-weighted images (TR2180 ms, TE72 ms). The layer thickness was 4 mm and the FOV matrix range was 138×256–172×320.

3. Experimental Data and Methods

3.1. Entropy Collected by MRI in 16 Normal Gastrocnemius Subjects in This Group. After the experiment is ready, the subjects will send the start message and hold the handle to keep the body balance but do not exert force. The body is perpendicular to the ground and the knees are not bent, and they start to raise the heel. The subjects are encouraged to try their best to reach the highest point and to fall to the lowest point without touching the ground. In the process of heel lifting, the speed should be kept as constant as possible and relatively slow to prevent experimental errors caused by unstable center of gravity or incorrect force generation caused by very fast lifting of the heel [5]. Impedance matching is achieved by filling a mixture between the skin surface and the array probe.

3.2. Maximum Strength Test of the Gastrocnemius Muscle. The maximum strength for 8 males and 8 females is shown in Table 1. It can be found that due to individual differences, the maximum strength of each subject is different. For each subject, the maximum force is the corresponding 100% force and the load is normalized on this basis as shown in Table 2.

3.3. Frequency of Calf Lifting with the Gastrocnemius Muscle. The experimental data collection was stopped when the calf began to shake and the heel lifting could not be completed fully [6]. The number of heel lifts of 8 males and 8 females is shown in Tables 3 and 4.

4. Results Analysis and Discussion

4.1. Entropy Fitting of MRI Images of the Gastrocnemius Muscle. MRI image acquisition of the fixed position of the calf gastrocnemius muscle of 16 subjects was processed with a computer to obtain the MRI image entropy value, and then, the fitting curve was obtained by using the least square method [7]. Figure 1 shows the fitting curves of 8 male subjects at no weight bearing, 20%MVCT, 30%MVCT, and 40%MVCT, respectively. Figure 2 shows the fitting curves of 8 female subjects at no weight bearing, 20%MVCT, 30% MVCT, and 40%MVCT, respectively. The abscissa is the number of heel lifts, and the ordinate is the entropy of MRI images.

4.2. Descending Slope of MRI Image Entropy of the Calf Gastrocnemius Muscle. After fitting the entropy values of the MRI images of the 16 subjects, the descending slope was summarized. The specific descending slope is shown in Table 5. During the process of raising the heel of each subject, the variation of MRI image entropy with the number

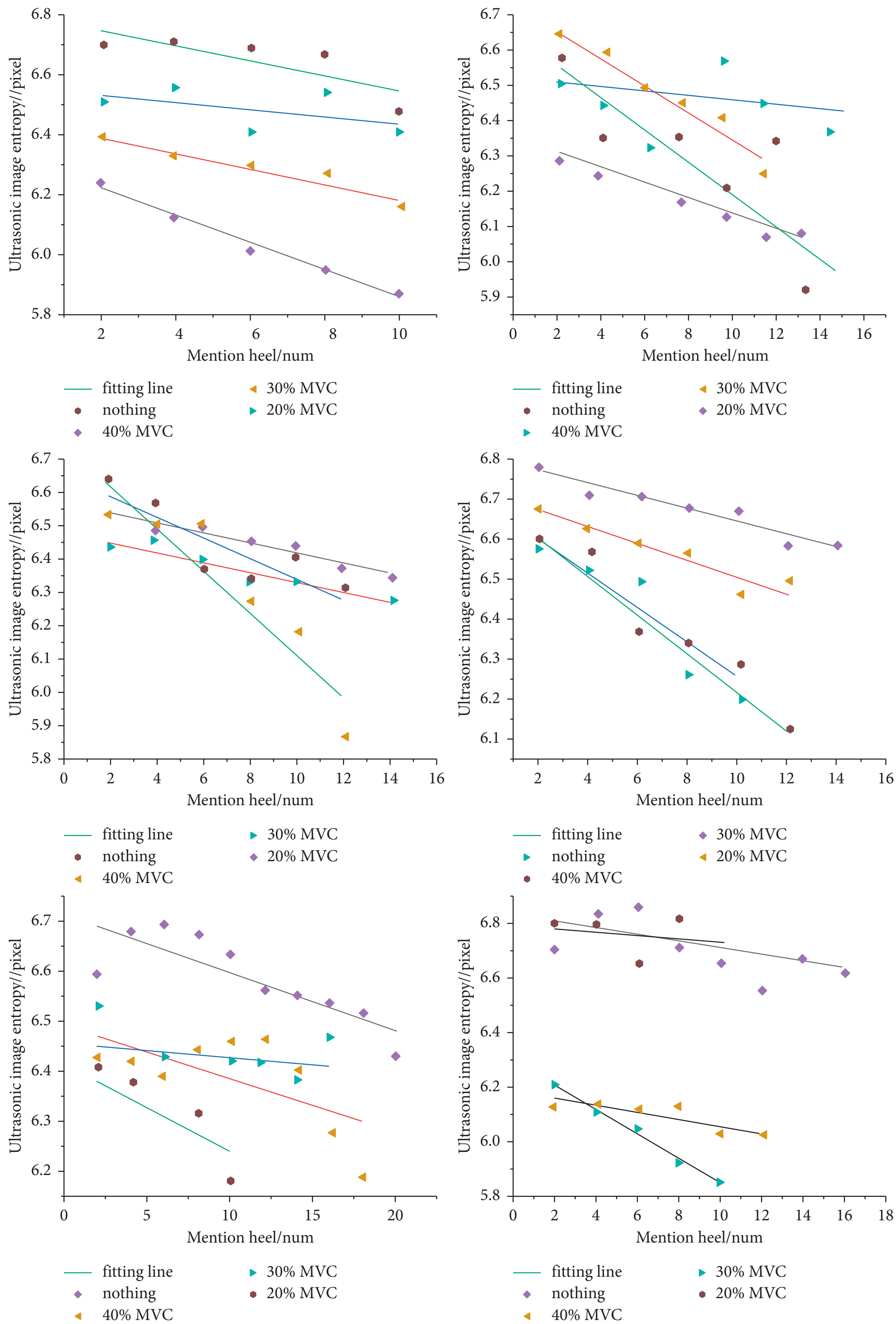

(a)

Figure 1: Continued.

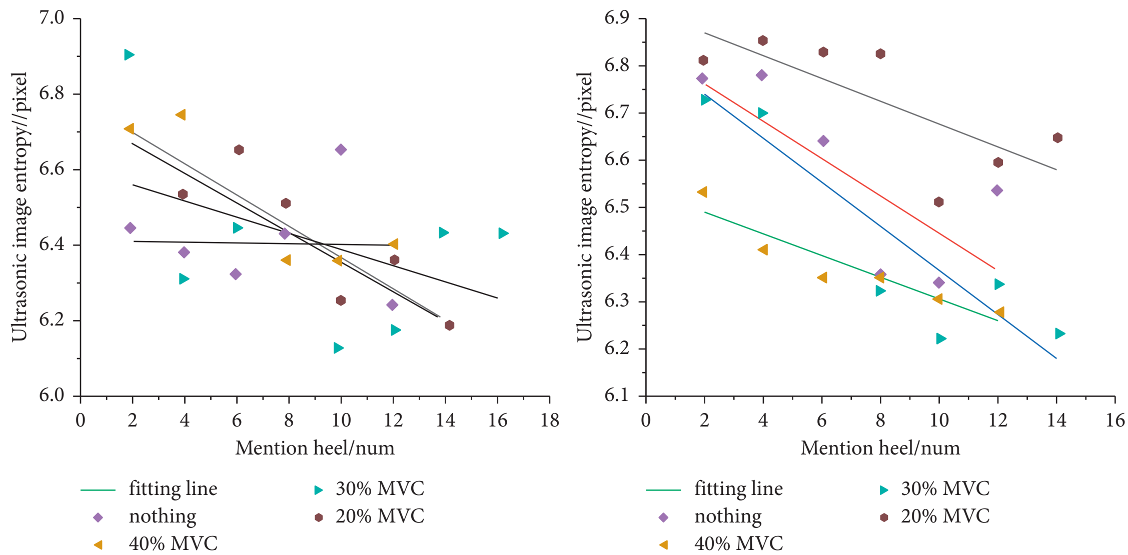

(b)

Figure 1: Entropy fitting diagram of MRI images of 8 male subjects under different loading conditions.

of heel lifts was measured under the conditions of no weight bearing, 20%MVCT, 30%MVCT, and 40%MCVT [8].

4.3. Relationship between the Descending Slope of Entropy of MRI Images of the Gastrocnemius Muscle and the Maximum Load. According to the descending slope of MRI image values of the calf gastrocnemius muscle under different loads summarized in Table 5 along with the number of heel lifts, the descending slope of MRI image entropy was taken as the abscess coordinate and the maximum load as the ordinate. The fitting figure is shown in Figure 3. Figure 3(a) shows 8 male subjects, and Figure 3(b) shows 8 female subjects. It can be found that there is a linear relationship between MRI image entropy and maximum load [9, 10].

It can be seen from Figures 1 and 2 that in the fitting line of MRI image entropy, with the increase in the number of heel lifts, muscle injury will occur, leading to the decrease in MRI image entropy. Through further control analysis, it can be seen that the larger the maximum voluntary contraction moment of male and female subjects in the injury process, the greater the descending slope of MRI image entropy, showing a significant negative correlation between the two.

4.4. One-Way ANOVA for MRI Image Entropy of Gastrocnemius. According to the descending slope of MRI image entropy in the process of calf gastrocnemius injury summarized in Table 5, the descending slope of MRI image entropy in the gastrocnemius muscle of 16 subjects was further analyzed by random block univariate analysis of variance. First, the relationship between the downward slope of MRI image entropy and gender was analyzed when muscle injury was caused by heel lifting under different weights. The slope of each weight bearing was divided into two groups, that is, 8 male subjects and 8 female subjects corresponding to different weights. Different torques were taken as the factors of this single-factor analysis of variance; secondly, the influence of weight bearing in the heel lifting exercise on the descending slope of MRI image entropy in the process of gastrocnemius muscle injury was analyzed. The descending slope of image entropy of 8 male subjects without weight bearing was taken as the first group, and so on. There were 4 groups in total, namely, no weight bearing, 20%MVCT, 30%MVCT, and 40%MCVT. Different genders were taken as the factors of this one-way ANOVA; that is, there were two different levels. Finally, the influence of individual differences of subjects on the descending slope of MRI image entropy was examined. Each subject was assigned to one block group, and there were 16 blocks in total. The statistical analysis process for this was completed by the single-way ANOVA module calculated by the SPSS analysis software, and the results obtained are shown in Table 6.

According to the descending slope of the MRI image entropy of 8 males and 8 females with the number of heel lifts above, one-way ANOVA was used to obtain the test results of the intersubject effect as shown in Table 4. When the source showed gender difference, the statistical identification values F were 1.891, 1.584, 0.651, and 0.852 at no weight bearing, 20%MVCT, 30%MVCT, and 40%MCVT, respectively, and the corresponding significance values P were 0.529, 0.188, 0.589, and 0.632, respectively. The significant values P were greater than 0.05, indicating that there was no significant difference in the decline slope of MRI image entropy between male and female subjects during heel lifting injury under the same load. When the source showed torque, the statistical identification value F of male subjects and female subjects was 0.736 and 0.957, respectively, and the corresponding statistical significance P was 0.542 and 0.351, respectively, both greater than 0.05, indicating that for

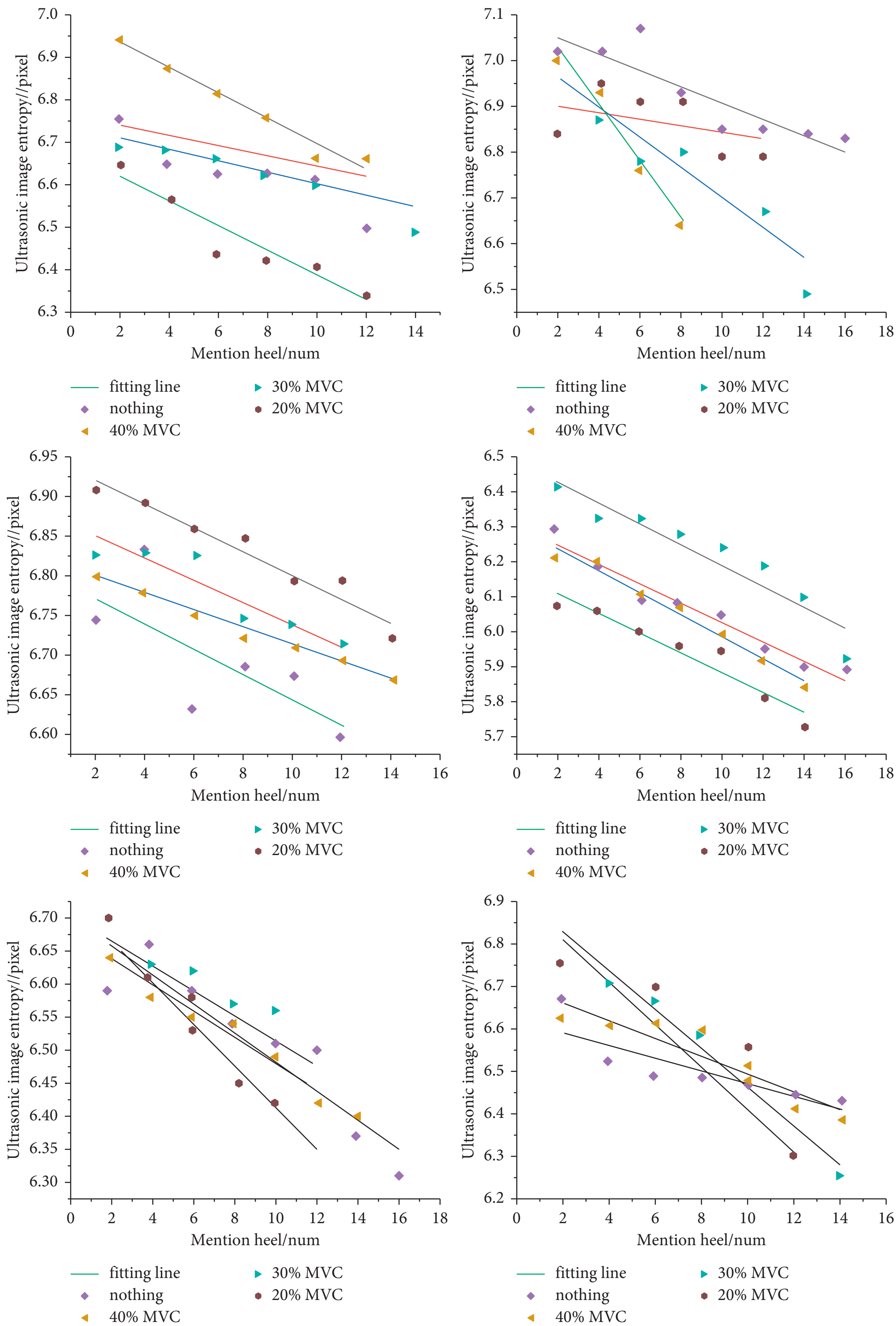

(a)

Figure 2: Continued.

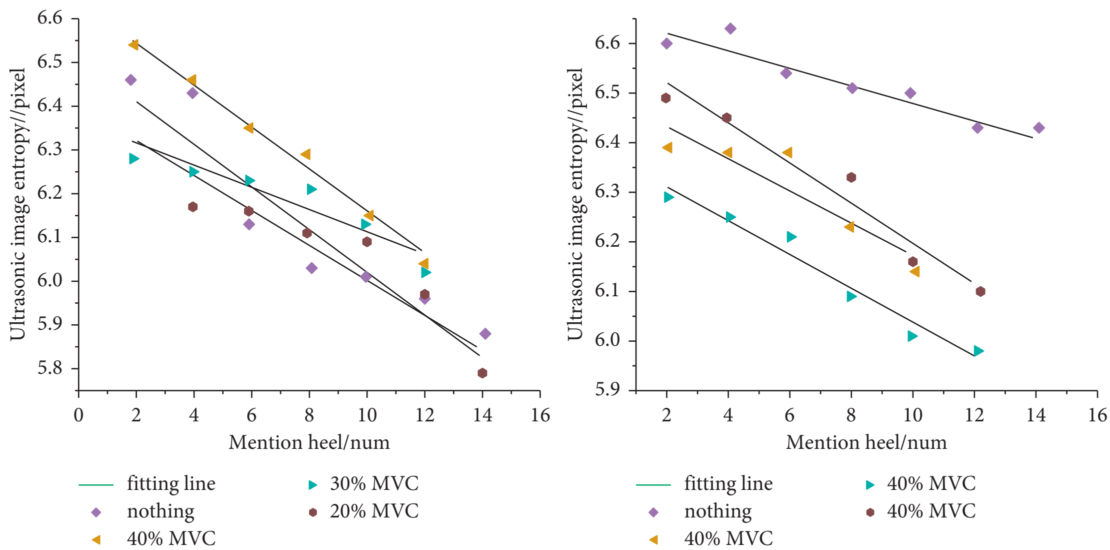

(b)

Figure 2: Entropy fitting diagram of MRI images of 8 female subjects under different weights.

Table 5: Descending slope of entropy of MRI images of the gastrocnemius muscle (unit: bit/pixel value).

Males	There is no load	20%MVCT	30%MVCT	40%MVCT	Slope mean
Subject 1	0.0056	0.0057	0.0072	0.0051	0.0059
Subject 2	0.0037	0.0038	0.0073	0.0055	0.0051
Subject 3	0.0093	0.0065	0.0028	0.0084	0.0067
Subject 4	0.0075	0.0075	0.0126	0.0177	0.0113
Subject 5	0.0146	0.0102	0.0150	0.0052	0.0112
Subject 6	0.0087	0.0074	0.0191	0.0140	0.0123
Subject 7	0.0126	0.0076	0.0200	0.0137	0.135
Subject 8	0.0089	0.0037	0.0083	0.0071	0.0070
Females	There is no load	20%MVCT	30%MVCT	40%MVCT	Slope mean
Subject 1	0.0057	0.0064	0.0053	0.0031	0.0051
Subject 2	0.0175	0.0132	0.0025	0.0101	0.0108
Subject 3	0.0150	0.0139	0.0056	0.0913	0.0315
Subject 4	0.123	0.0124	0.0126	0.0106	0.0120
Subject 5	0.0428	0.0489	0.0827	0.0111	0.0464
Subject 6	0.0078	0.0100	0.0063	0.0104	0.0086
Subject 7	0.0109	0.0111	0.0396	0.0133	0.0187
Subject 8	0.0213	0.0189	0.0072	0.0198	0.0168

all male subjects and all female subjects, when the weight of heel lifting is different, there was no significant difference in the descending slope of MRI entropy of the gastrocnemius muscle. When the source showed subject difference, the statistical identification value F of male subjects and female subjects was 7.526 and 1.286, respectively, and the corresponding statistical significance P was 0.000 and 0.000, respectively, both less than 0.05. This indicates that different subjects have significant differences in the descending slope of image entropy in the process of injury caused by weight-bearing heel lifting [11].

5. Results of Surface EMG Signals

In this experiment, MRI images of the calf gastrocnemius muscle during heel lifting were collected and synchronous surface EMG signals were also collected. The surface EMG signals of each subject with heel lifting under different weights were segmented at their intersection points, respectively processed to obtain the corresponding root mean square (RMS), and then normalized and fitted by the least square method under different forces of different subjects. Figure 4 is the fitting schematic diagram of the surface EMG

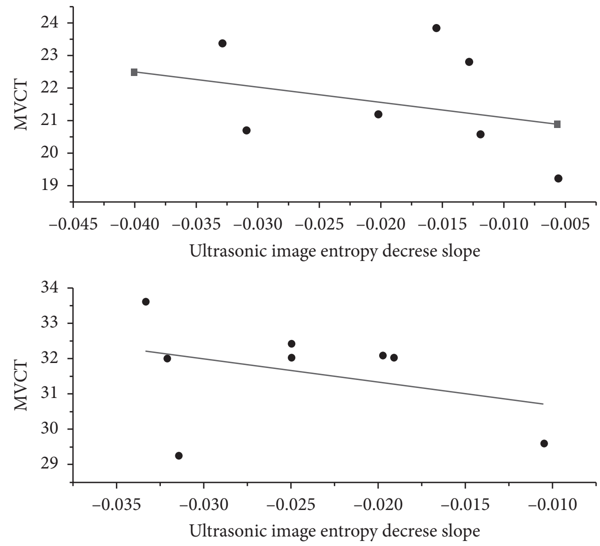

Figure 3: Relationship between the descending slope of MRI images of 16 subjects and the maximum load.

Table 6: One-way ANOVA results.

Source		Sum of squares	df	Average	F	Sig.
Gender differences	There is no load	0.000	1	0.000	1.891	0.529
	20%MVCT	0.001	1	0.000	1.584	0.188
	30%MVCT	0.004	1	0.002	.651	0.589
	40%MVCT	0.000	1	0.001	.852	0.632
Torque difference	Males	0.001	3	0.000	.736	0.542
	Females	0.003	3	0.001	.957	0.351
Subject difference	Males	0.002	7	0.000	7.526	0.000
	Females	0.004	7	0.007	1.286	0.000

signals of one male (top) and one female (bottom) at different moments. The abscissa is the experimental time, and the ordinate is the normalized root mean square value.

Figure 4 is a fitting plot of root mean square values for one male subject and one female subject with the same trend for the rest of the subjects. Table 7 shows the statistical results of the descending slope after fitting the root mean square values of all subjects.

Through the overall analysis, it can be found that in the process of calf gastrocnemius muscle lifting, the root mean square value of surface EMG of the target muscle presents an increasing trend, which is consistent with the results of previous studies. It shows that in this experiment, the gastrocnemius muscle did undergo the injury process after the calf lifting.

The multichannel surface electromyography of each subject under different loads was analyzed. The abscissa of the multichannel surface electromyography represented the root mean square of the downhill slope and the root mean square of the uphill slope as the ordinate. The least square fitting of the slope change relationship was used to represent the relationship between the two in the MRI image entropy. The slope of the line after fitting is shown in Table 8.

Through the above results, it can be found that, by analyzing the decline slope of MRI image entropy in the process of injury, the rise slope of normalized root mean square of multichannel sEMG in previous studies can be characterized. With the increase of load, the degree of negative correlation between them becomes larger and larger, but in general, the slope of men is greater than that of women.

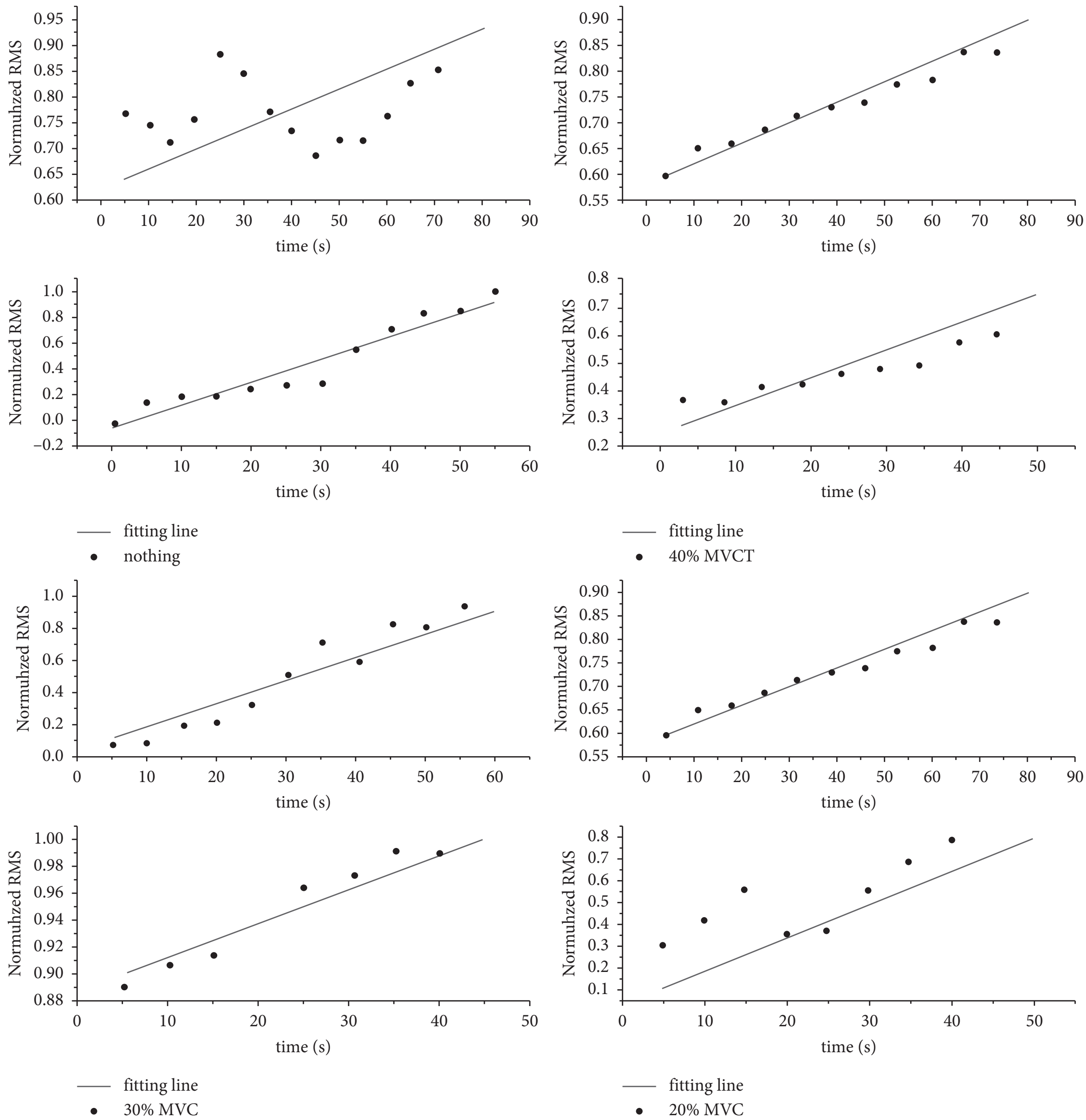

Figure 4: Normalized RMS values of surface EMG signals of subjects at different torques.

Table 7: Fitting slope of the RMS values of the surface EMG signals of 16 subjects.

Males	There is no load	20%MVCT	30%MVCT	40%MVCT	Slope mean
Subject 1	0.0056	0.0057	0.0072	0.0051	0.0059
Subject 2	0.0037	0.0038	0.0073	0.0055	0.0051
Subject 3	0.0093	0.0065	0.0028	0.0084	0.0067
Subject 4	0.0075	0.0075	0.0126	0.0177	0.0113
Subject 5	0.0146	0.0102	0.0150	0.0052	0.0112
Subject 6	0.0087	0.0074	0.0191	0.0140	0.0123
Subject 7	0.0126	0.0076	0.0200	0.0137	0.135
Subject 8	0.0089	0.0037	0.0083	0.0071	0.0070
Females	There is no load	20%MVCT	30%MVCT	40%MVCT	Slope mean
Subject 1	0.0057	0.0064	0.0053	0.0031	0.0051
Subject 2	0.0175	0.0132	0.0025	0.0101	0.0108
Subject 3	0.0150	0.0139	0.0056	0.0913	0.0315
Subject 4	0.123	0.0124	0.0126	0.0106	0.0120
Subject 5	0.0428	0.0489	0.0827	0.0111	0.0464
Subject 6	0.0078	0.0100	0.0063	0.0104	0.0086
Subject 7	0.0109	0.0111	0.0396	0.0133	0.0187
Subject 8	0.0213	0.0189	0.0072	0.0198	0.0168

Table 8: Relationship between the rising slope of surface EMG signal and the descending slope of MRI image entropy.

	There is no load	20%MVCT	30%MVCT	40%MVCT	The average
Males	0.1461	0.0957	0.0374	0.0635	0.7959
Females	−0.0242	−0.2996	−0.04161	−1.373	0.118

6. Conclusions

Muscle injuries and muscle damage diseases are closely related to our daily life, especially in the mass movement trend, under the guidance of people exercising actively; especially, the athletes in the training process are more prone to muscle damage. When people receive professional training because of reasons that their strength is not correct or need more degrees of training, this also greatly increases the risk of sports injury. In the process of exercise, people may ignore the decline of the body movement ability, leading to muscle injury. If they continue to exercise at this time, they will get muscle strain. In serious cases, professional athletes will suffer from muscle injury and other consequences, which will affect people's daily life and the training effect of professional athletes. Therefore, it is of great significance to understand and evaluate muscle injury to improve physique and enhance athletic ability.

Therefore, this paper proposes a method for the preliminary prediction of muscle injury. In this paper, the increase of the root mean square of surface EMG signals of the gastrocnemius muscle in the process of heel lifting was used to prove that the denser gastrocnemius muscle actually experienced injury and reached the injury state after lifting the heel. By obtaining the images of the gastrocnemius muscle in the process of heel lifting, the MRI images of the subjects during the whole movement process were obtained. After fitting with the least square method, the descending slope of the image moisture value was obtained, which was used as a parameter to evaluate the state of muscle injury. This paper presents a convenient, real-time, and noninvasive method for the assessment of muscle tissue injury. Subsequent work should be done to increase the number of experimental samples and physiological and biochemical indicators to accurately evaluate the relationship between the percentage of decreased MRI images and the degree of injury.

There are still some shortcomings in this paper, which will be improved in the next study. In the follow-up study, professional athletes will be selected as subjects, the number of subjects will be increased, the exercise mode will be increased, and physiological and biochemical indicators will be added to evaluate the injury degree of different muscle groups.

Data Availability

The data used to support the findings of this study are available from the corresponding author upon request.

Conflicts of Interest

The author declares no conflicts of interest.

References

[1] K. Mizutani, J. Atsuta, T. Shibata, E. Azuma, and M. Sakurai, "Consecutive cerebral mri findings of acute relapsing disseminated encephalomyelitis," *Pediatrics International*, vol. 36, no. 6, pp. 709–712, 2015.

[2] A. Serner, A. Weir, J. L. Tol et al., "Can standardised clinical examination of athletes with acute groin injuries predict the presence and location of mri findings?" *British Journal of Sports Medicine*, vol. 50, no. 24, pp. 1541–1547, Article ID 096290, 2016.

[3] T. A. Herschmiller, J. A. Anderson, W. E. Garrett, and D. C. Taylor, "The trapped medial meniscus tear: an examination maneuver helps predict arthroscopic findings," *Orthopaedic Journal of Sports Medicine*, vol. 3, no. 5, Article ID 2325967115583954, 2015.

[4] E. Rio and D. A. Opar, "Lower limb injury: improving our translation of research into clinical practice for acute injuries and long-term sequelae," *British Journal of Sports Medicine*, vol. 49, no. 10, p. 635, 2015.

[5] T. Gustafsson, A. H. Östenberg, and M. Alricsson, "ACL diagnosis - the correlation between Rolimeter and MRI," *Sports Orthopaedics and Traumatology*, vol. 36, no. 3, pp. 278–283, 2020.

[6] R. P. Mathew, R. S. Basti, P. Hegde, J. M. Devdas, H. U. Khan, and M. J. Bukelo, "Rare case of acute dengue encephalitis with correlated mri findings," *Journal of Medical Imaging & Radiation Oncology*, vol. 58, no. 6, pp. 679–682, 2015.

[7] K. E. Hoque, C. J. Myers, M. Law, and P. Kim, "Mri brain findings of intravenous iron therapy," *Neurographics*, vol. 7, no. 1, pp. 61–63, 2017.

[8] G. Foti, W. Mantovani, M. Catania, P. Avanzi, S. Caia, and C. Zorzi, "Evaluation of glenoid labral tears: comparison between dual-energy ct arthrography and mr arthrography of the shoulder," *La radiologia medica*, vol. 125, no. 1, pp. 39–47, 2020.

[9] L. M. Hoessly and M. L. Wildi, "Magnetic resonance imaging findings in the knee before and after long-distance running—documentation of irreversible structural damage? a systematic review," *The American Journal of Sports Medicine*, vol. 45, no. 5, pp. 1206–1217, 2017.

[10] É. C. Falvey, E. King, S. Kinsella, and A. Franklyn-Miller, "Athletic groin pain (part 1): a prospective anatomical diagnosis of 382 patients—clinical findings, mri findings and patient-reported outcome measures at baseline," *British Journal of Sports Medicine*, vol. 50, no. 7, pp. 423–430, 2016.

[11] H. Lee, X. Zhao, H. K. Song, and F. W. Wehrli, "Self-navigated three-dimensional ultrashort echo time technique for motion-corrected skull mri," *IEEE Transactions on Medical Imaging*, vol. 39, no. 99, p. 1, 2020.